

# High density symmetric nuclear matter in the Bethe-Brueckner-Goldstone approach

M. Baldo,<sup>1,\*</sup> A. Fiasconaro,<sup>2</sup> H. Q. Song,<sup>3,4,5</sup> G. Giansiracusa,<sup>2</sup> and U. Lombardo<sup>2</sup>

<sup>1</sup>*INFN, Sezione di Catania, 57 Corso Italia, I-95129 Catania, Italy*

<sup>2</sup>*Dipartimento di Fisica and INFN, 57 Corso Italia, I-95129 Catania, Italy*

<sup>3</sup>*Institute of Nuclear Research, Academia Sinica, Shanghai 201800, China*

<sup>4</sup>*CCAST (World Laboratory), P.O. Box 8730, Beijing 100080, China*

<sup>5</sup>*Center of Theoretical Physics, National Laboratory of Heavy Ion Accelerator, Lanzhou 730000, China*

(Received 3 May 2001; published 13 December 2001)

Previous calculations of the equation of state of symmetric nuclear matter, with the inclusion of the three-hole-line contribution, are extended to densities up to about six times the saturation value. The calculations are performed for the Argonne  $v_{14}$  and the Argonne  $v_{18}$  two-nucleon potentials, and a larger set of partial waves is included. Evidence for the convergence of the Bethe-Brueckner-Goldstone expansion, even at relatively high density, is presented. The contribution to the equation of state of the three-hole-line diagrams, within the continuous choice of the single-particle potential, turns out to be almost negligible, except at the highest densities.

DOI: 10.1103/PhysRevC.65.017303

PACS number(s): 21.65.+f, 21.30.Fe, 21.60.Gx

## I. INTRODUCTION

The equation of state (EOS) of nuclear matter at high density is one of the relevant issues in the theory of neutron star structure, and it is the object of intensive studies in the physics of heavy-ion collisions at intermediate energies. The theoretical calculations of the EOS needs a full many-body treatment, since a major role is played by the strong nucleon-nucleon short range correlations, which is a distinct feature of nuclear matter.

Recently [1,2], we have shown that the Bethe-Brueckner-Goldstone (BBG) expansion in nuclear matter converges at the three-hole level of approximation for neutron and symmetric nuclear matter. The results turned out to be largely independent of the choice of the self-consistent single-particle potential, which is indeed a clear sign of convergence. The calculations were performed for densities up to about six times the saturation value for pure neutron matter, while the analysis for symmetric nuclear matter was restricted to densities not greater than  $0.4 \text{ fm}^{-3}$ . In this Brief Report we will extend the analysis for symmetric nuclear matter to higher densities and we will also study the relevance of including a larger set of partial waves.

The BBG expansion can be ordered according to the number of independent hole lines appearing in the diagrams, representing the different terms of the expansion. This grouping of diagrams generates the so-called hole-line expansion [3,4]. At the two-hole-line level of approximation the corresponding summation of diagrams produces the Brueckner-Hartree-Fock (BHF) approximation, which is expected to incorporate the main contribution from the two-particle correlations. The BHF approximation includes the self-consistent procedure of determining the single-particle auxiliary potential, which is an essential ingredient of the method. The choice of the single-particle potential is, however, not unique. In principle the single-particle potential is

an auxiliary potential that is introduced only to improve the convergence of the expansion, and it is therefore, to a certain extent, arbitrary. The “potential insertion” diagrams take into account the corresponding modifications of the expansion for a given choice of the auxiliary potential.

Since the early works on BBG theory of nuclear matter, many papers have been devoted to the effects produced by the possible choices of the single-particle potentials [5,6]. They were mainly based on the resummation of diagrams corresponding to insertions, both in hole and particle lines, which produce energy shifts in the denominators of simpler diagrams [6]. A choice that had become quite popular is based on the self-consistent definition the single-particle potential  $U(k)$  in terms of the scattering  $G$  matrix, see Eq. (2) below, with the restriction that  $U(k)$  was set equal to zero for particle states, i.e., for momenta  $k$  larger than the Fermi momentum  $k_F$ . Since then the single-particle energy has a gap at the Fermi momentum, this choice is referred to as “gap choice.” The presence of a gap appears unphysical, and therefore in more modern calculations  $U(k)$  is taken to be continuous through the Fermi surface, by extending the same self-consistent procedure also above  $k_F$ . This second choice is usually called “continuous choice.” The final result of a hypothetically exact BBG calculation is independent of the auxiliary potential chosen, but the rate of convergence can of course depend on the particular choice adopted. Among the different possible choices of  $U(k)$  we shall restrict the analysis to these two choices, since they represent somehow two opposite extreme cases.

The three-hole-line diagrams can be summed up by solving the Bethe-Faddeev equations for the three-body scattering matrix inside nuclear matter. As shown by Rajaraman and Bethe [7], the summation is essential, since individual three-hole-line diagrams can be quite large, but substantial cancellation occurs once the whole set of three-hole diagrams is considered.

The two-hole and three-hole diagrams are depicted in Fig. 1, where a wavy line represents a Brueckner  $G$  matrix. In the

\*Corresponding author. Email address: baldo@ct.infn.it

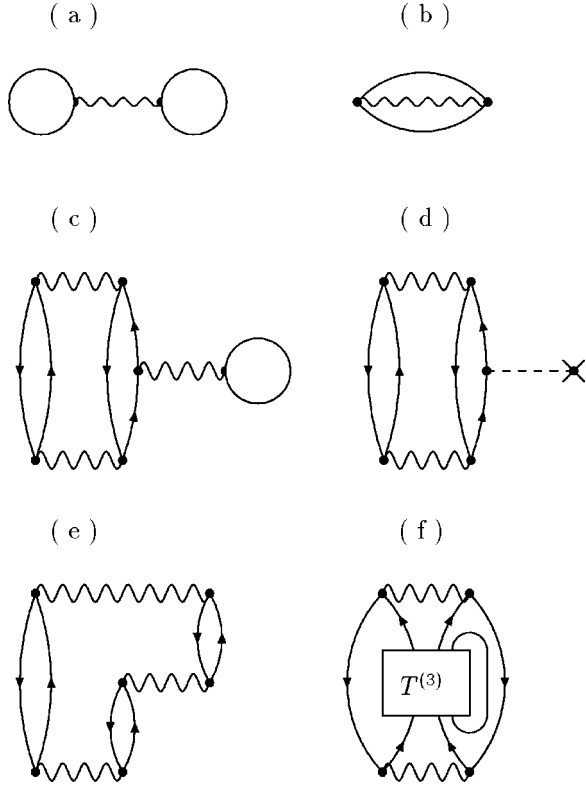


FIG. 1. Two-hole-line diagrams (a),(b) and three-hole-line diagrams (c)–(f) in the Bethe-Brueckner-Goldstone expansion. A wavy line indicates a Brueckner  $G$  matrix. Diagram (f) indicates schematically the whole set of three-hole-line diagrams in terms of the three-body scattering matrix  $T^{(3)}$ . The “bubble” diagram (c) and the “ring” diagram (e) are the lowest-order ones in the number of  $G$  matrix, i.e., they are obtained from diagram (f) by replacing  $T^{(3)}$  with a single  $G$  matrix (direct and exchange terms). Finally, the potential insertion diagram (d) is present only for the continuous choice. See the text for further details.

schematic diagram of Fig. 1(f), the box  $T^{(3)}$  indicates the irreducible three-body scattering matrix, namely, it does not include the first-order (one  $G$  matrix) contributions. The latter, if formally inserted in the diagram in place of the  $T^{(3)}$  box, give rise to the so called “bubble” and “ring” diagrams, depicted separately in Figs. 1(c) and 1(e), respectively. They are singled out from the whole set of three-hole-line diagrams for computational convenience only. In the case of the continuous choice, the additional “potential insertion” diagram of Fig. 1(d) has to be included, since in this case  $U(k)$  is different from zero also for single-particle momenta  $k > k_F$ . In principle, the expansion includes also the two diagrams in which the bubble and the potential insertions are attached to a hole line. However, they cancel out each other exactly, because of the Bethe-Brandow-Petschek theorem [8], for both choices of the auxiliary potential  $U(k)$ .

## II. FORMALISM

The summation of the two-hole diagrams can be performed by solving the integral equation for the Brueckner  $G$  matrix

$$\begin{aligned} \langle k_1 k_2 | G(\omega) | k_3 k_4 \rangle &= \langle k_1 k_2 | v | k_3 k_4 \rangle + \sum_{k'_3 k'_4} \langle k_1 k_2 | v | k'_3 k'_4 \rangle \\ &\times \frac{[1 - \Theta_F(k'_3)][1 - \Theta_F(k'_4)]}{\omega - e_{k'_3} - e_{k'_4}} \langle k'_3 k'_4 | G(\omega) | k_3 k_4 \rangle, \end{aligned} \quad (1)$$

where  $\Theta_F(k) = 1$  for  $k < k_F$  and is zero otherwise. The product  $Q(k, k') = [1 - \Theta_F(k)][1 - \Theta_F(k')]$ , appearing in the kernel of Eq. (1), enforces the scattered momenta to lie outside the Fermi sphere, and it is commonly referred as the “Pauli operator.” This  $G$  matrix can be viewed as the in-medium scattering matrix between two nucleons. The  $G$  matrix depends parametrically on the entry energy  $\omega$ , namely it is defined in general also off-shell, as the usual scattering matrix in vacuum. The self-consistent single-particle potential  $U(k)$  is determined by the equation

$$U(k) = \sum_{k' < k_F} \langle k k' | G(e_k + e_{k'}) | k k' \rangle_A, \quad (2)$$

where  $|k k' \rangle_A = |k k' \rangle - |k' k \rangle$  and  $e_k = \hbar^2 k^2 / 2m + U(k)$  is the single-particle energy. This definition of  $e_k$ , together with Eqs. (1) and (2), implies the above-mentioned self-consistent procedure for  $U(k)$ . In the gap choice the definition of Eq. (2) is restricted to  $k < k_F$ . Once the single-particle potential  $U(k)$  and the  $G$  matrix are calculated, the two-hole-line contribution  $E_2$  to the energy is then given by

$$E_2 = \frac{1}{2} \sum_{k_1, k_2 < k_F} \langle k_1 k_2 | G(e_{k_1} + e_{k_2}) | k_1 k_2 \rangle_A. \quad (3)$$

Similarly, the summation of the three-hole-line diagrams can be performed by solving the integral equation for the three-body scattering matrix, the Bethe-Faddeev equation [3,7]. It reads schematically

$$T^{(3)} = G + GX \frac{Q_3}{e} T^{(3)},$$

$$\begin{aligned} \langle k_1 k_2 k_3 | T^{(3)} | k'_1 k'_2 k'_3 \rangle &= \langle k_1 k_2 | G | k'_1 k'_2 \rangle \delta_k(k_3 - k'_3) \\ &+ \left\langle k_1 k_2 k_3 \left| GX \frac{Q_3}{e} T^{(3)} \right| k'_1 k'_2 k'_3 \right\rangle. \end{aligned} \quad (4)$$

The factor  $Q_3/e$  is the analogous of the similar factor appearing in the integral equation for the two-body scattering matrix  $G$ ; see Eq. (1). Therefore, the projection operator  $Q_3$  imposes that all the three-particle states lie above the Fermi energy, and the denominator  $e$  is the appropriate energy denominator, namely, the energy of the three-particle intermediate state minus the entry energy  $\omega$ , in close analogy with the equation for the two-body scattering matrix  $G$  of Eq. (1). The real novelty with respect to the two-body case is the operator  $X$ , which imposes that the  $G$  matrices must alternate from one pair of particle lines to another, in all possible

ways, to avoid double counting of the ladder series defining the  $G$  matrix. It is important to realize that the three-hole-line diagrams describe the *irreducible* part of the three-nucleon correlations, i.e., the ones that cannot be reduced to products of two-body correlations. Indeed, the many-body wave function at the Brueckner level contains already many-body correlations to all orders, which can be written as independent products of two-body correlations [4].

Finally, in terms of the three-body scattering matrix  $T^{(3)}$  the contribution  $E_3$  of the three-hole-line diagrams to the energy is given by

$$E_3 = \frac{1}{2} \sum_{k_1, k_2, k_3 \leq k_F} \sum_{\{k'\}, \{k''\} \geq k_F} \langle k_1 k_2 | G | k'_1 k'_2 \rangle_A \times \frac{1}{e} \langle k'_1 k'_2 k_3 | X T^{(3)} X | k''_1 k''_2 k_3 \rangle \frac{1}{e} \langle k''_1 k''_2 | G | k_1 k_2 \rangle_A. \quad (5)$$

An exchange term has to be added, which is obtained by multiplying with an extra operatorial factor  $X$  the expression of Eq. (5).

### III. RESULTS AND CONCLUSIONS

The self-consistent  $G$ -matrix equation (1) has been solved for both the continuous and gap choices for the Argonne  $v_{14}$  [9] and  $v_{18}$  [10] potentials. The set of two-body partial waves was extended until convergence was reached also for the highest density. The potential  $U(k)$  was numerically evaluated up to a certain cutoff  $k_c$  and kept constant then after ( $k > k_c$ ). The value of  $k_c$  was increased until the results appeared insensitive to a further increase. The value  $k_c \approx 7.5 \text{ fm}^{-1}$  was found appropriate. Once the single-particle potential  $U(k)$  has been obtained, the corresponding single-particle spectrum was used in solving the Bethe-Faddeev equations. Also in this case we checked the convergence with respect to the number of two-body and three-body channels included in the calculations of the three-hole-line diagrams. More details on the numerical procedure will be given elsewhere.

In Fig. 2(a) the symmetric nuclear matter equation of state is reported for the Argonne  $v_{18}$  potential. The full lines indicate the energy per particle as a function of the Fermi momentum  $k_F$  at the Brueckner two-hole-line level of approximation, for the gap (BHF-G) and continuous (BHF-C) choices. The main difference between the results obtained with the two possible choices is the stronger stiffness of the EOS in the continuous choice. The reason for this behavior can be due to the effect of the single-particle potential (see Fig. 3), which becomes repulsive at large momenta. This effect is obviously absent in the gap choice, since in this case the potential is set equal to zero above the Fermi momentum. The sizable difference between the two EOS at the Brueckner level indicates that the convergence cannot be yet considered satisfactory. If the contribution of the three-hole-line diagrams is added, one obtains the EOS marked by the open squares and the open circles in the gap and continuous

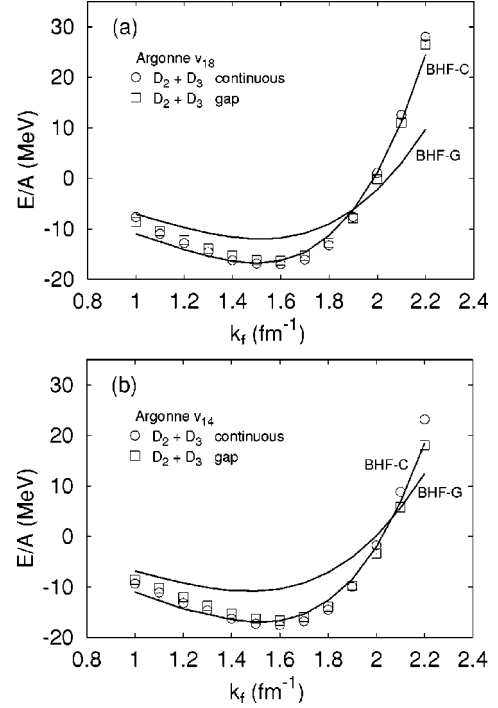


FIG. 2. (a) The equation of state of symmetric nuclear matter for the Argonne  $v_{18}$  potential. The full lines indicate the result at the Brueckner two-hole-line level of approximation, for the gap (BHF-G) and the continuous (BHF-C) choices. The full EOS, including the three-hole-line contribution, is labeled by the open squares and the open circles for the gap and continuous choices, respectively. (b) The same as in (a), but for the Argonne  $v_{14}$  potential.

choices, respectively. The two EOS are now in much closer agreement for the whole range of densities, which is a strong indication that convergence has been reached to a good accuracy. As it is apparent from the figure, the three-hole-line contribution turns out to be much smaller in the continuous than in the gap choice. The smallness of the three hole-line contributions is a further indication of convergence. Similar results hold for the  $v_{14}$  potential [see Fig. 2(b)].

The three-hole-line contribution in the continuous choice is indeed almost negligible, except at the highest density, and oscillates around zero with a maximum absolute value of about 2 MeV. Despite the smallness of the contribution, the trend of the three-hole-line contribution shows some difference with respect to the results reported in Ref. [1]. This is due to the larger single-particle momentum cutoff and the larger number of partial waves used in the present calculations. It has to be stressed, anyway, that the final EOS are very close to the previous ones of Ref. [1], where the calculations were performed for the Argonne  $v_{14}$  potential and restricted to Fermi momenta  $k_F \leq 1.8 \text{ fm}^{-1}$ . This shows that the calculations have reached a satisfactory numerical stability. One can also notice that the discrepancy in the EOS between the two considered potentials, which is sizable at the Brueckner two-hole-line level of approximation, is substantially reduced when the three-hole-line contribution is added. Therefore, the final EOS are quantitatively quite similar for the two nucleon-nucleon potentials.

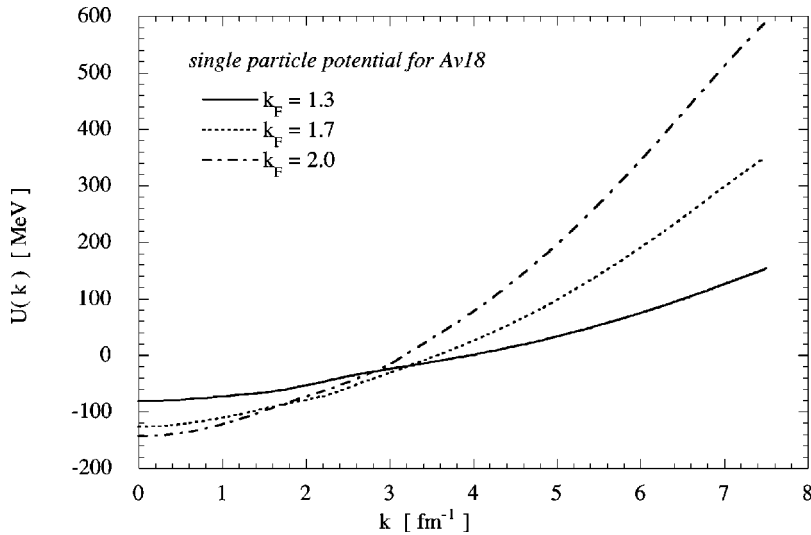


FIG. 3. The single-particle self-consistent potentials as a function of momentum at different densities and for the Argonne  $v_{18}$  two-nucleon potential.

Comparison with the variational calculations of Ref. [12] in the case of the two-body Argonne  $v_{18}$  potential shows a fair agreement. However, the variational EOS is systematically below the BBG saturation curve, in particular at higher densities, where the discrepancy reaches few MeV. The discrepancy needs further studies to be clarified.

In conclusion, we have shown that the BBG expansion in symmetric nuclear matter is convergent to good accuracy up to about six times the saturation density, for both the Argonne  $v_{14}$  and Argonne  $v_{18}$  potentials. The resulting EOS do not reproduce the empirical saturation point, since, as it is well known, realistic two-body forces are not able to reproduce the correct saturation point, in line with the results obtained in light nuclei; see Ref. [11] for recent Monte Carlo

“exact” calculations. Three-body forces are most likely the main term missing in the nuclear Hamiltonian. Also relativistic effects introduced by the Dirac-Brueckner model can be interpreted as due to a particular three-body force [13]. Therefore, the inclusion of three-body forces is mandatory. Within the BBG expansion this has been done only at the two-hole-line level [14]. At the three-hole-line level, one should solve the Bethe-Faddeev equations with three-body forces included. The value of the wound parameter [2] and early estimates within the Bethe-Faddeev equations [15] seem to indicate a minor correction to the EOS due to the three-body forces at the three-hole-line level. However, this should be checked again with modern two- and three-body interactions. This is left to future work.

- 
- [1] H. Q. Song, M. Baldo, G. Giansiracusa, and U. Lombardo, Phys. Rev. Lett. **81**, 1584 (1998).  
 [2] M. Baldo, G. Giansiracusa, U. Lombardo, and H. Q. Song, Phys. Lett. B **473**, 1 (2000).  
 [3] For a pedagogical introduction, see *Nuclear Methods and the Nuclear Equation of State*, edited by M. Baldo (World Scientific, Singapore, 1999), International Review of Nuclear Physics, Vol. 9.  
 [4] B. D. Day, in *Proceedings of the School E. Fermi*, Varenna 1981, Course LXXIX, edited by A. Molinari (Editrice Compositori, Bologna, 1983), pp. 1–72; Rev. Mod. Phys. **39**, 719 (1967).  
 [5] K. A. Brueckner and J. L. Gammel, Phys. Rev. **105**, 1679 (1957); **109**, 1023 (1958); S. A. Coon and J. Dabrowski, Phys. Rev. **140**, B287 (1965).  
 [6] H. S. Kohler, Nucl. Phys. **A204**, 65 (1973); Phys. Rep., Phys. Lett. **18C**, 217 (1975).  
 [7] R. Rajaraman and H. Bethe, Rev. Mod. Phys. **39**, 745 (1967).  
 [8] H. A. Bethe, B. H. Brandow, and A. G. Petschek, Phys. Rev. **129**, 225 (1962).  
 [9] R. B. Wiringa, R. A. Smith, and T. L. Ainsworth, Phys. Rev. C **29**, 1207 (1984).  
 [10] R. B. Wiringa, V. G. J. Stocks, and R. Schiavilla, Phys. Rev. C **51**, 38 (1995).  
 [11] Steven C. Pieper, V. R. Pandharipande, R. B. Wiringa, and J. Carlson, nucl-th/0102004; Steven C. Pieper and R. B. Wiringa, nucl-th/0103005; Ann. Rev. Nucl. Part. Sci. (to be published).  
 [12] A. Akmal, V. R. Pandharipande, and D. G. Ravenhall, Phys. Rev. C **58**, 1804 (1998).  
 [13] G. E. Brown, W. Weise, G. Baym, and J. Speth, Comments Nucl. Part. Phys. **17**, 39 (1987).  
 [14] M. Baldo, I. Bombaci, and G. F. Burgio, Astron. Astrophys. **328**, 274 (1997).  
 [15] R. I. Jibuti and R. Ya. Kezerashvili, in *Issledovania po Teorii Structuri Yader* (Metsniereba, Tbilisi, 1974)